Title

Superalkali Coated Rydberg Molecules.

Authors

Tkachenko, Nikolay
Rublev, Pavel
Boldyrev, Alexander
et al.

Publication Date
2022

DOI
10.3389/fchem.2022.880804

frontiers | Frontiers in Chemistry

ORIGINAL RESEARCH
published: 13 April 2022
doi: 10.3389/fchem.2022.880804

Superalkali Coated Rydberg Molecules

Nikolay V. Tkachenko[1], **Pavel Rublev**[1], **Alexander I. Boldyrev**[1]* **and Jean-Marie Lehn**[2]

[1]Department of Chemistry and Biochemistry, Utah State University, Logan, UT, United States, [2]Laboratoire de Chimie Supramoléculaire, Institut de Science et d'Ingénierie, Supramoléculaires Université de Strasbourg, Strasbourg, France

A series of complexes of Na, K, NH_4, and H_3O with [bpy.bpy.bpy]cryptand, [2.2.2] cryptand, and spherical cryptand were investigated *via* DFT and ab initio methods. We found that by coating Rydberg molecules with the "organic skin" one could further decrease their ionization potential energy, reaching the values of ~1.5 eV and a new low record of 1.3 eV. The neutral cryptand complexes in this sense possess a weakly bounded electron and may be considered as very strong reducing agents. Moreover, the presence of an organic cage increases the thermodynamic stability of Rydberg molecules making them stable toward the proton detachment.

Keywords: cryptands, cryptatium, superalkalis, Rydberg molecules, ionization potential (IP)

OPEN ACCESS

Edited by:
Suzana Velickovic,
University of Belgrade, Serbia

Reviewed by:
Cina Foroutan-Nejad,
Institute of Organic Chemistry (PAN), Poland
Jose Luis Cabellos,
Polytechnic University of Tapachula, Mexico

****Correspondence:***
Alexander I. Boldyrev
a.i.boldyrev@usu.edu

Specialty section:
This article was submitted to Physical Chemistry and Chemical Physics,
a section of the journal Frontiers in Chemistry

Received: *21 February 2022*
Accepted: *14 March 2022*
Published: *13 April 2022*

Citation:
Tkachenko NV, Rublev P, Boldyrev AI and Lehn J-M (2022) Superalkali Coated Rydberg Molecules. Front. Chem. 10:880804. doi: 10.3389/fchem.2022.880804

INTRODUCTION

The [2.2.2]cryptand and spherical cryptand (**Scheme 1A, B**) invented by Lehn (Lehn, 1977), have been a subject of both theoretical (Elroby et al., 2006; Elroby, 2009; Puchta et al., 2019; Isaeva et al., 2021; Ćoćić et al., 2021; Ariyarathna, 2022) and experimental (Lehn, 1977; Lehn, 1978; Lehn, 1979; Lehn, 1980; Echegoyen et al., 1991; Arnaud-Neu et al., 2002; Cram et al., 2002; Izatt et al., 2002; Miyamoto et al., 2002; Badjić et al., 2011; Chung et al., 2020) studies for decades. The discovery of those fascinating compounds opened a huge field of supramolecular chemistry. Their unique guest particle selectivity and extremely low ionization potentials of neutral alkali-metal complexes (Cram and Lein, 1985; Huang et al., 1988; Kim et al., 1999) found an application in synthetic organic and inorganic chemistry. In particular, a huge number of multiply-charged Zintl anions with unusual structures have been synthesized using the popular [K⊂[2.2.2]cryptand] complex (Sun et al., 2018; Tkachenko et al., 2020; Wang et al., 2020).

Firstly, introduced by Gutsev and Boldyrev (Gutsev and Boldyrev, 1982), the family of superalkalis has been growing significantly. Despite the initially proposed $M_{k+1}L$ family, where M is an alkali atom and L is an electronegative atom of valence k, other superalkalis have been proposed and synthesized. Along with other inorganic binuclear superalkali (Tong et al., 2009), the definition of superalkalis was extended to polynuclear species such as polynuclear aromatic superalkalis (Sun et al., 2013; Parida et al., 2018), superalkali cations (Tong et al., 2011; Tong et al., 2012a; Tong et al., 2012b; Hou et al., 2013), organo-Zintl clusters (Giri et al., 2016; Reddy and Giri, 2016). Another family of compounds with low ionization potential is Rydberg molecules. Vivid examples of Rydberg molecules are NH_4 and H_3O neutral species, whose unpa`ired electron occupies a diffuse orbital around the molecule. It has been shown that such Rydberg molecules are not long-living particles. Although the T_d structure of NH_4 radical is a local minimum, it is only a metastable molecule and undergoes a dissociation into NH_3 and H* radical species (Herzberg, 1981; Signorell et al., 1997). Similar behavior is found for H_3O neutral species (Luo and Jungen, 1999; Melin et al., 2005). It has been shown before that cryptand compounds can bind both NH_4^+ and H_3O^+ cations with a great selectivity (Cram et al., 1985; Behr et al., 2002; Junk, 2008). Thus, it will be interesting to

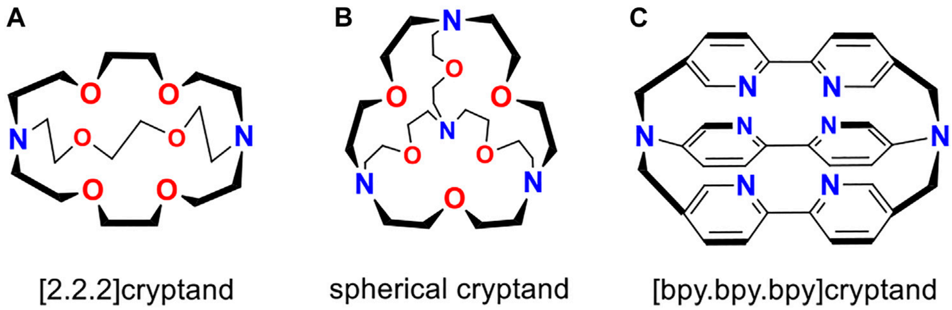

SCHEME 1 | The structures of organic cages considered in this work. [2.2.2]cryptand **(A)**, spherical cryptand **(B)**, and [bpy.bpy.bpy]cryptand **(C)** are shown.

investigate the electronic properties of neutral [R⊂cryptand] (R = NH_4, H_3O) complexes, since the organic coating could stabilize the Rydberg molecules and decrease their ionization potential as it was observed for alkali metal complexes (Cram and Lein, 1985; Huang et al., 1988; Kim et al., 1999). In this work, we investigate the electronic properties of coated Rydberg molecules *via* DFT and *ab initio* methods and compare their properties with alkali-metal cryptand complexes.

COMPUTATIONAL METHODS

All structures were optimized using Perdew–Burke-Ernzerhof (PBE0) (Perdew et al., 1996) and Tao-Perdew-Staroverov-Scuseria (TPSSh) (Staroverov et al., 2003) hybrid functionals using def2-SVP basis set (Weigend and Ahlrichs, 2005). The frequency calculations were performed at the same level of theory. No imaginary frequencies were present, showing that the optimized structures are at local minima on the given PES. Ionization potentials were calculated at three different levels of theory. In particular, the single-point calculations at optimized geometry using DFT functionals (PBE0 and TPSSh) and a moderately large basis set def2-TZVPPD (Weigend and Ahlrichs, 2005) were carried out. In addition, single-point calculations using MP2 level of theory with cc-pvdz (C, N, O atoms) and aug-cc-pvdz (H, K, Na atoms) basis sets (Dunning, 1989; Kendall et al., 1992; Hill and Peterson, 2017) were performed. For convenience, we will denote this combination of basis functions as *Basis-1*. Due to the large values of spin contamination, the [bpy.bpy.bpy]cryptand complexes were calculated using ROHF-MBPT2 formalism (Lauderdale et al., 1991; Lauderdale et al., 1992). The vertical ionization potential (VIP) was calculated as the energy difference between the optimized neutral complex and the cation in the geometry of the neutral complex. The adiabatic ionization potential (AIP) was calculated as the energy differences between an optimized neutral cluster and an optimized cation. The natural charge distribution was calculated via NBO method as implemented in NBO7 software (Glendening et al., 2019). The topology analysis of electron localization function (ELF) (Silvi and Savin, 1994) was performed with the Multiwfn program (Lu and Chen, 2012). All calculations were performed with Gaussian 16 program (Frisch et al., 2016). The visualization of SOMO orbitals and geometries of the investigated species were performed using IboView software (Knizia, 2013; Knizia and Klein, 2015).

RESULTS AND DISCUSSION

The neutral [Na⊂[bpy.bpy.bpy]cryptand] was firstly synthesized in 1991 by Lehn and coworkers (Echegoyen et al., 1991) through the electrochemical reduction of [Na^+⊂[bpy.bpy.bpy]cryptand] cation. This approach potentially can be used for the synthesis of superalkali cryptand complexes with Rydberg molecules. To investigate the electronic properties of such species, we chose three different organic cages ([2.2.2]cryptand, [bpy.bpy.bpy] cryptand, and spherical cryptand) that are very promising candidates for the capturing of NH_4 and H_3O species. The structures of those cages are given in **Scheme 1**. For the comparison of ionization potentials, two alkali metal complexes were also considered. In particular [Na⊂[bpy.bpy.bpy]cryptand] was chosen as the first synthesized cryptand-superalkali species, and [K⊂[2.2.2]cryptand] was chosen as one of the most popular examples of alkali metal macrocyclic complex.

The geometries of neutral and cationic complexes were optimized with two different DFT hybrid functionals. It was shown before that PBE0 and TPSSh functionals can provide accurate geometries for macrocyclic and cryptand complexes (Tkachenko et al., 2019). The optimized geometries are consistent within two methods, showing the functional independence of the results. The geometries of neutral species are only slightly distorted from the geometries of cationic species, showing that the additional electron of neutral complexes does not participate in a significant

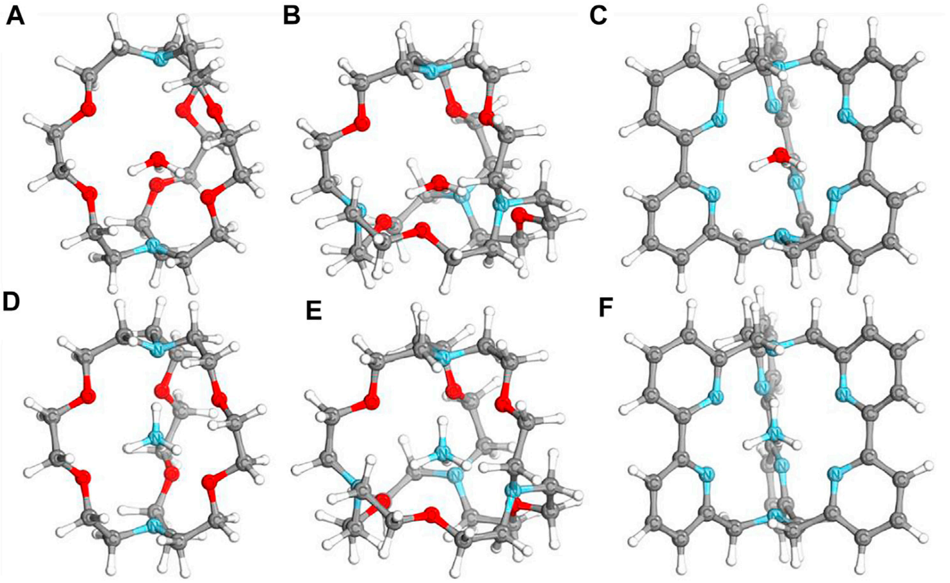

FIGURE 1 | Structures of optimized neutral complexes of NH_4 and H_3O. **(A)** [H_3O⊂[2.2.2]cryptand]; **(B)** [H_3O⊂spherical cryptand]; **(C)** [H_3O⊂[bpy.bpy.bpy] cryptand]; **(D)** [NH_4⊂[2.2.2]cryptand]; **(E)** [NH_4⊂spherical cryptand]; **(F)** [NH_4⊂[bpy.bpy.bpy]cryptand].

TABLE 1 | Free energies [kcal/mol] for the dissociation reaction of hydrogen radical from the central unit of investigated species calculated at TPSSh/def2-TZVPPD//TPSSh/def2-SVP level.

Species	ΔG_r	Species	ΔG_r
NH_4	−12.98	H_3O	−21.94
[NH_4⊂spherical cryptand]	24.61	[H_3O⊂spherical cryptand]	−6.43
[NH_4⊂[2.2.2]cryptand]	17.10	[H_3O⊂[2.2.2]cryptand]	−26.00
[NH_4⊂[bpy.bpy.bpy]cryptand]	52.98	[H_3O⊂[bpy.bpy.bpy]cryptand]	32.55

bonding formation process. The optimized structures of selected neutral species are given in **Figure 1**. Cartesian coordinates of all optimized structures are provided in the Supporting Information file (**Supplementary Table S1**). The natural charge distribution of neutral species showed that the negative charge is mainly distributed over the oxygen and nitrogen atoms of the organic ligand, while the central unit (either H_3O or NH_4 species) formally possesses a +1 positive charge. In particular 0.757–0.806 and 0.794–0.876 positive natural charges on H_3O and NH_4 molecules, respectively, were found in investigated complexes. This might be one of the key reasons for the stabilization of those Rydberg molecules, which are thermodynamically unstable toward dissociation of a proton in their naked form.

To illustrate the enhanced stability of encapsulated neutral molecules we performed calculations of dissociation energies for both naked and coated species. The reaction that was considered is a dissociation of a proton from the central unit with a formal reaction: $AH^{\bullet} \rightarrow A + H^{\bullet}$. Energies were calculated using the following expression: $\Delta G_r = \Delta G(A) + \Delta G(H^{\bullet}) - \Delta G(AH^{\bullet})$. The results are shown in **Table 1**. As we can observe, the dissociation of naked H_3O and NH_4 occurs with a significant release of energy (21.9 and 13.0 kcal/mol, respectively). While the dissociation of the same species coated by cryptand complexes is energetically not favorable for most of the compexes (**Table 1**). Such a difference in ΔG_r values can lead us to the conclusion that [R⊂cryptand] complexes are thermodynamically more stable species, which may open the possibility of their fabrication.

Interestingly, for both NH_4 and H_3O, a significant decrease in ionization potentials was found after encapsulating the corresponding Rydberg molecules into organic cages. Particularly, the naked NH_4 and H_3O molecules possess 4.57 and 5.55 eV VIP, respectively. Whereas the NH_4 and H_3O encapsulated in [2.2.2]cryptand and spherical cryptand possess ionization potentials about 3–4 eV lower than the naked species (**Table 2**). Interestingly [bpy.bpy.bpy]cryptand systems show larger IPs by ~1.1 eV. A similar but not so pronounced pattern was found for alkali metals encapsulated in the [bpy.bpy.bpy]cryptand. The nature of such an increase in IPs is discussed below and related to the presence of a diffuse SOMO orbital in the system. We note, that the obtained IPs for NH_4 and H_3O species are even lower than

TABLE 2 | Values of VIP and AIP [eV] obtained at MP2/*Basis-1* level of theory.

Species	AIP	VIP	Species	AIP	VIP
Na	N/A	4.961	[NH_4⊂spherical cryptand]	1.358	1.389
K	N/A	4.072	[NH_4⊂[2.2.2]cryptand]	1.308	1.381
NH_4	4.429	4.566	[NH_4⊂[bpy.bpy.bpy]cryptand]	2.385	2.582
H_3O	5.310	5.552	[H_3O⊂spherical cryptand]	1.379	1.696
[Na⊂[bpy.bpy.bpy]cryptand]	2.440	2.729	[H_3O⊂[2.2.2]cryptand]	1.362	1.676
[K⊂[2.2.2]cryptand]	1.387	1.612	[H_3O⊂[bpy.bpy.bpy]cryptand]	2.501	2.729

TABLE 3 | Values of VIP and AIP [eV] obtained using PBE0 and TPSSh functionals with def2-TZVPPD basis set.

Species	PBE0		TPSSh	
	AIP	VIP	AIP	VIP
K	N/A	4.370	N/A	4.233
Na	N/A	5.280	N/A	5.152
NH_4	4.417	4.584	4.313	4.462
H_3O	5.384	5.964	5.343	5.606
[NH_4⊂spherical cryptand]	1.440	1.519	1.400	1.479
[NH_4⊂[2.2.2]cryptand]	1.445	1.537	1.403	1.504
[NH_4⊂[bpy.bpy.bpy]cryptand]	3.060	3.220	3.214	3.359
[H_3O⊂ spherical cryptand]	1.457	1.780	1.388	1.704
[H_3O⊂[2.2.2]cryptand]	1.387	1.821	1.492	1.638
[H_3O⊂[bpy.bpy.bpy]cryptand]	3.162	3.323	3.307	3.452
[Na⊂[bpy.bpy.bpy]cryptand]	3.157	3.335	3.298	3.407
[K⊂[2.2.2]cryptand]	1.811	1.830	1.784	1.803

IPs of [K⊂[2.2.2]cryptand] which was shown before to be a superalkali with record low ionization potential (Tkachenko et al., 2019).

Similar results were obtained using PBE0 and TPSSh functionals with def2-TZVPPD basis set. Although the values of IPs are slightly higher than it was obtained for the MP2 method, the main trends preserve the same (**Table 3**).

To illustrate the diffuse nature of SOMO of investigated species, we plotted the isosurface graphs of corresponding orbitals shown in **Figure 2** (the orbitals were obtained from quasi-restricted orbitals formalism). We can see that for [2.2.2] cryptand and spherical cryptand complexes (**Figures 2A,B,D,E**), SOMO orbitals have a diffuse nature and surround the whole molecule entirely. In contrast, the unpaired electron of [bpy.bpy.bpy]cryptand complexes sit on the antibonding orbital of a π-conjugated system (**Figures 2C,F**). Isosurface plots of SOMO visualized with a different contour value can be found in the supporting information file (**Supplementary Figure S1**). Such an interesting difference in SOMO can be explained by the fact that different organic cages form different types of complexes with Rydberg molecules. Thus [2.2.2]cryptand and spherical

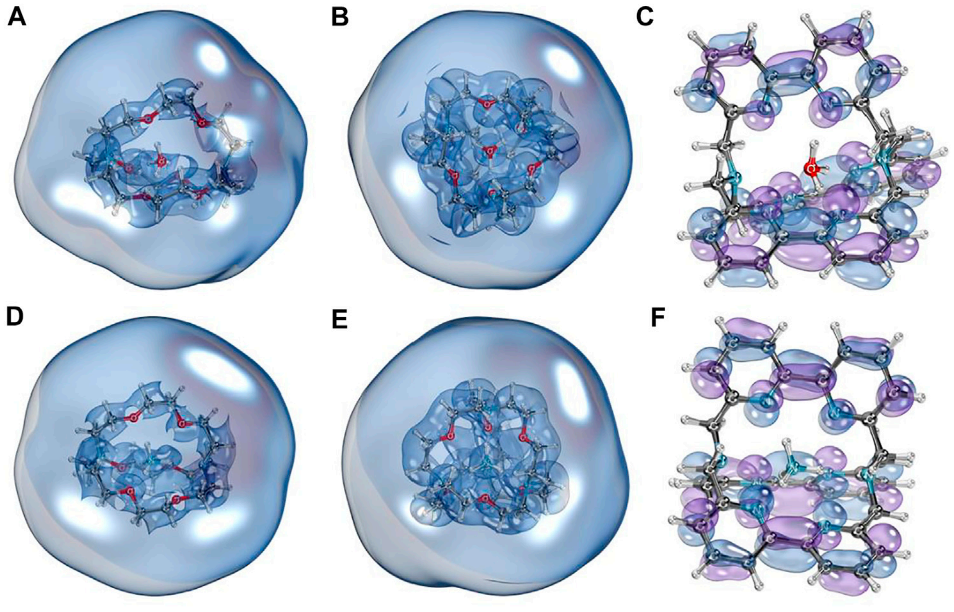

FIGURE 2 | Isosurface plots of singly occupied molecular orbitals of NH_4 and H_3O complexes. **(A)** [H_3O⊂[2.2.2]cryptand]; **(B)** [H_3O⊂spherical cryptand]; **(C)** [H_3O⊂[bpy.bpy.bpy]cryptand]; **(D)** [NH_4⊂[2.2.2]cryptand]; **(E)** [NH_4⊂spherical cryptand]; **(F)** [NH_4⊂[bpy.bpy.bpy]cryptand]. A threshold of 100% was used for A, B, D, E to illustrate the diffuse nature of those orbitals. For C and F a lower 80% threshold was used for visualization.

cryptand complexes behave as electrides, possessing an electron density outside of the molecule, whereas [bpy.bpy.bpy]cryptand complexes form an ionic molecular compound bearing a negative charge entirely on the organic ligand. Such behavior can also be explained by the possibility of bipyridine molecules to form stable anionic species, that were experimentally isolated before (Bock et al., 1999; Gore-Randall et al., 2009). To further show the differences between the two types of complexes we performed an ELF basins analysis. The basins laying outside of the molecule were found for [2.2.2]cryptand and spherical cryptand complexes (**Supplementary Figure S2**). The integration of the electron density within the volume of the found ELF basins resulted in 0.3–0.6 |e| basins occupancy. In turn, no outside lying ELF basins were found for [bpy.bpy.bpy]cryptand complexes. Thus [2.2.2]cryptand and spherical cryptand complexes demonstrate an electride nature which is the reason for their lower IP values in comparison to [bpy.bpy.bpy] cryptand complexes.

CONCLUSION

In this work we investigated the electronic properties of Rydberg molecules coated with cryptand organic cages. We showed that it is possible to significantly decrease the values of the ionization potentials by covering Rydberg molecules with an “organic skin.” In particular, we found that the IP could be decreased, reaching the values of ~1.5 eV and a new low record of 1.3 eV (at MP2/*Basis-1* level). In addition, the coating ligand can increase the thermodynamic stability of a Rydberg molecule, opening an opportunity to obtain such strong reducing agents in the experiment.

DATA AVAILABILITY STATEMENT

The additional data that support the findings of this study are available from the corresponding author on a reasonable request.

AUTHOR CONTRIBUTIONS

All authors listed have made a substantial, direct, and intellectual contribution to the work and approved it for publication. NVT and PR performed the quantum chemical calculations and analyzed the data. AIB and JML conceived and designed the project.

FUNDING

AIB acknowledges financial support from the R. Gaurth Hansen Professorship fund.

ACKNOWLEDGMENTS

The support and resources from the Centre for High Performance Computing at the University of Utah are gratefully acknowledged. The authors thank the reviewer 1 for proposing a discussion on electride nature of [2.2.2]cryptand and spherical cryptand complexes.

SUPPLEMENTARY MATERIAL

The Supplementary Material for this article can be found online at: https://www.frontiersin.org/articles/10.3389/fchem.2022.880804/full#supplementary-material

REFERENCES

Ariyarathna, I. R. (2022). Superatomic Chelates: The Cases of Metal Aza-Crown Ethers and Cryptands. *Inorg. Chem.* 61 (1), 579–585. doi:10.1021/ACS.INORGCHEM.1C03261

Arnaud-Neu, F., Spiess, B., and Schwing-Weill, M. J. (2002). Solvent Effects in the Complexation of [2]-Cryptands and Related Monocycles with Transition- and Heavy-Metal Cations. *J. Am. Chem. Soc.* 104 (21), 5641–5645. doi:10.1021/JA00385A014

Badjić, J. D., Stojanović, S., and Ruan, Y. (2011). Kinetically and Thermodynamically Controlled Syntheses of Covalent Molecular Capsules. *Adv. Phys. Org. Chem.* 45, 1–37. doi:10.1016/B978-0-12-386047-7.00001-1

Behr, J. P., Dumas, P., and Moras, D. (2002). The Oxonium (H_3O^+) Cation: Molecular Structure of an Oxonium-Macrocyclic Polyether Complex. *J. Am. Chem. Soc.* 104 (17), 4540–4543. doi:10.1021/JA00381A007

Bock, H., Lehn, J. M., Pauls, J., Holl, S., Krenzel, V., Rousset, C. J., et al. (1999). Sodium Salts of the Bipyridine Dianion: Polymer $[(bpy)^{2-}\{Na^+(dme)\}_2]\infty$, Cluster $[(Na_8O)^{6+}\ Na^+{}_6(bpy)^{2-}{}_6\ (Tmeda)_6$, and Monomer $[(bpy)^{2-}\{Na^+(Pmdta)\}_2]$. *Angew. Chem. Intl Edit* 38 (7), 952–955. doi:10.1002/(sici)1521-3773(19990401)38:7<952:aid-anie952>3.0.co;2-#

Chung, A. B., Huh, D. N., Ziller, J. W., and Evans, W. J. (2020). 2.2.2-Cryptand as a Bidentate Ligand in Rare-Earth Metal Chemistry. *Inorg. Chem. Front.* 7 (22), 4445–4451. doi:10.1039/D0QI00746C

Ćoćić, D., Manaa, A., Siegl, S., Puchta, R., and Eldik, R. (2021). [3.2.1] and [4.1.1] Isomers of Lehn’s [2.2.2] Cryptand: Prediction of Ion Selectivity by Quantum Chemical Calculations XV**. *Z. Anorg. Allg. Chem.* 647 (8), 915–921. doi:10.1002/ZAAC.202000452

Cram, D. J., Kaneda, T., Helgeson, R. C., Brown, S. B., Knobler, C. B., Maverick, E., et al. (1985). Host-guest Complexation. 35. Spherands, the First Completely Preorganized Ligand Systems. *J. Am. Chem. Soc.* 107 (12), 3645–3657. doi:10.1021/JA00298A040

Cram, D. J., Kaneda, T., Helgeson, R. C., and Lein, G. M. (2002). Spherands - Ligands Whose Binding of Cations Relieves Enforced Electron-Electron Repulsions. *J. Am. Chem. Soc.* 101 (22), 6752–6754. doi:10.1021/JA00516A048

Cram, D. J., and Lein, G. M. (1985). Host-guest Complexation. 36. Spherand and Lithium and Sodium Ion Complexation Rates and Equilibria. *J. Am. Chem. Soc.* 107 (12), 3657–3668. doi:10.1021/JA00298A041

Dunning, T. H. (1989). Gaussian Basis Sets for Use in Correlated Molecular Calculations. I. The Atoms boron through Neon and Hydrogen. *J. Chem. Phys.* 90 (2), 1007–1023. doi:10.1063/1.456153

Echegoyen, L., DeCian, A., Fischer, J., and Lehn, J.-M. (1991). Cryptatium: A Species of Expanded Atom/Radical Ion Pair Type from Electroreductive Crystallization of the Macrobicyclic Sodium Tris(Bipyridine) Cryptate. *Angew. Chem. Int. Ed. Engl.* 30 (7), 838–840. doi:10.1002/ANIE.199108381

Elroby, S. A. K. (2009). The Effect of Donor Atoms on the Complexation of Alkali Cations with Spherands: A Density Functional Investigation. *Int. J. Quan. Chem.* 109 (7), 1515–1521. doi:10.1002/QUA.21970

Elroby, S. A., Lee, K. H., Cho, S. J., and Hinchliffe, A. (2006). A DFT Study of Spherands Containing Five Anisyl Groups - Highly Preorganized to Bind the Alkali Metal. *Can. J. Chem.* 84 (8), 1045–1049. doi:10.1139/V06-130

Frisch, M. J., Trucks, G. W., Schlegel, H. B., Scuseria, G. E., Robb, M. A., Cheeseman, J. R., et al. (2016). *Gaussian 16, Revision B.01.* Wallingford, CT: Gaussian, Inc.

Giri, S., Reddy, G. N., and Jena, P. (2016). Organo-Zintl Clusters [P_7R_4]: A New Class of Superalkalis. *J. Phys. Chem. Lett.* 7 (5), 800–805. doi:10.1021/ACS.JPCLETT.5B02892/SUPPL_FILE/JZ5B02892_LIVESLIDES.MP4

Glendening, E. D., Landis, C. R., and Weinhold, F. (2019). NBO 7.0 : New Vistas in Localized and Delocalized Chemical Bonding Theory. *J. Comput. Chem.* 40 (25), 2234–2241. doi:10.1002/JCC.25873

Gore-Randall, E., Irwin, M., Denning, M. S., and Goicoechea, J. M. (2009). Synthesis and Characterization of Alkali-Metal Salts of 2,2′- and 2,4′-Bipyridyl Radicals and Dianions. *Inorg. Chem.* 48 (17), 8304–8316. doi:10.1021/IC9009459

Gutsev, G. L., and Boldyrev, A. I. (1982). DVM X_α Calculations on the Electronic Structure of "superalkali" Cations. *Chem. Phys. Lett.* 92 (3), 262–266. doi:10.1016/0009-2614(82)80272-8

Herzberg, G. (1981). Rydberg Spectra of Triatomic Hydrogen and of the Ammonium Radical. *Faraday Discuss. Chem. Soc.* 71 (0), 165–173. doi:10.1039/DC9817100165

Hill, J. G., and Peterson, K. A. (2017). Gaussian Basis Sets for Use in Correlated Molecular Calculations. XI. Pseudopotential-Based and All-Electron Relativistic Basis Sets for Alkali Metal (K-Fr) and Alkaline Earth (Ca-Ra) Elements. *J. Chem. Phys.* 147 (24), 244106. doi:10.1063/1.5010587

Hou, N., Li, Y., Wu, D., and Li, Z.-R. (2013). Do Nonmetallic Superalkali Cations Exist? *Chem. Phys. Lett.* 575, 32–35. doi:10.1016/J.CPLETT.2013.05.014

Huang, R. H., Faber, M. K., Moeggenborg, K. J., Ward, D. L., and Dye, J. L. (1988). Structure of K^+(cryptand[2.2.2]) Electride and Evidence for Trapped Electron Pairs. *Nature* 331 (6157), 599–601. doi:10.1038/331599a0

Isaeva, V. A., Gamov, G. A., and Sharnin, V. A. (2021). Quantum-Chemical Calculations and Stability Analysis of Copper(II) Complexes with Cryptand [2.2.2]. *Russ. J. Inorg. Chem.* 66 (11), 1696–1702. doi:10.1134/S0036023621110097

Izatt, R. M., Bradshaw, J. S., Nielsen, S. A., Lamb, J. D., Christensen, J. J., and Sen, D. (2002). Thermodynamic and Kinetic Data for Cation-Macrocycle Interaction. *Chem. Rev.* 85 (4), 271–339. doi:10.1021/CR00068A003

Junk, P. C. (2008). Crown Ethers as Stabilising Ligands for Oxonium Ions. *New J. Chem.* 32 (5), 762–773. doi:10.1039/B800122G

Kendall, R. A., Dunning, T. H., and Harrison, R. J. (1992). Electron Affinities of the First-row Atoms Revisited. Systematic Basis Sets and Wave Functions. *J. Chem. Phys.* 96 (9), 6796–6806. doi:10.1063/1.462569

Kim, J., Ichimura, A. S., Huang, R. H., Redko, M., Phillips, R. C., Jackson, J. E., et al. (1999). Crystalline Salts of Na^- and K^- (Alkalides) that Are Stable at Room Temperature. *J. Am. Chem. Soc.* 121 (45), 10666–10667. doi:10.1021/JA992667V

Knizia, G. (2013). Intrinsic Atomic Orbitals: An Unbiased Bridge between Quantum Theory and Chemical Concepts. *J. Chem. Theor. Comput.* 9 (11), 4834–4843. doi:10.1021/CT400687B

Knizia, G., and Klein, J. E. M. N. (2015). Electron Flow in Reaction Mechanisms-Revealed from First Principles. *Angew. Chem. Int. Ed.* 54 (18), 5518–5522. doi:10.1002/ANIE.201410637

Lauderdale, W. J., Stanton, J. F., Gauss, J., Watts, J. D., and Bartlett, R. J. (1991). Many-body Perturbation Theory with a Restricted Open-Shell Hartree—Fock Reference. *Chem. Phys. Lett.* 187 (1–2), 21–28. doi:10.1016/0009-2614(91)90478-R

Lauderdale, W. J., Stanton, J. F., Gauss, J., Watts, J. D., and Bartlett, R. J. (1992). Restricted Open-shell Hartree-Fock-based Many-body Perturbation Theory: Theory and Application of Energy and Gradient Calculations. *J. Chem. Phys.* 97 (9), 6606–6620. doi:10.1063/1.463664

Lehn, J.-M. (1979). Macrocyclic Receptor Molecules: Aspects of Chemical Reactivity. Investigations into Molecular Catalysis and Transport Processes. *Pure Appl. Chem.* 51 (5), 979–997. doi:10.1351/PAC197951050979

Lehn, J. M. (1980). Cryptate Inclusion Complexes, Effects on Solute-Solute and Solute-Solvent Interactions and on Ionic Reactivity. *Pure Appl. Chem.* 52 (10), 2303–2319. doi:10.1351/PAC198052102303

Lehn, J. M. (1978). Cryptates: Inclusion Complexes of Macropolycyclic Receptor Molecules. *Pure Appl. Chem.* 50 (9–10), 871–892. doi:10.1351/PAC197850090871

Lehn, J. M. (1977). Cryptates: Macropolycyclic Inclusion Complexes. *Pure Appl. Chem.* 49 (6), 857–870. doi:10.1351/PAC197749060857

Lu, T., and Chen, F. (2012). Multiwfn: A Multifunctional Wavefunction Analyzer. *J. Comput. Chem.* 33 (5), 580–592. doi:10.1002/JCC.22885

Luo, M., and Jungen, M. (1999). The H_3O Rydberg Radical. *Chem. Phys.* 241 (3), 297–303. doi:10.1016/S0301-0104(98)00426-1

Melin, J., Ortiz, J. V., Martín, I., Velasco, A. M., and Lavín, C. (2005). Ground and Excited States of the Rydberg Radical H_3O: Electron Propagator and Quantum Defect Analysis. *J. Chem. Phys.* 122 (23), 234317. doi:10.1063/1.1926286

Miyamoto, R., Sato, H., and Sudoh, S. (2002). EPR Spectral Study of Gadolinium(III) Cryptate. *EPR in the 21st Century* 2002, 316–321. doi:10.1016/B978-044450973-4/50058-5

Parida, R., Reddy, G. N., Ganguly, A., Roymahapatra, G., Chakraborty, A., and Giri, S. (2018). On the Making of Aromatic Organometallic Superalkali Complexes. *Chem. Commun.* 54 (31), 3903–3906. doi:10.1039/C8CC01170B

Perdew, J. P., Burke, K., and Ernzerhof, M. (1996). Generalized Gradient Approximation Made Simple. *Phys. Rev. Lett.* 77 (18), 3865–3868. doi:10.1103/PHYSREVLETT.77.3865

Puchta, R., Ćoćić, D., Michel, M., and van Eldik, R. (2019). Host-guest Complexes of the Beer-Can-Cryptand: Prediction of Ion Selectivity by Quantum Chemical Calculations XI. *J. Coord. Chem.* 72 (12), 2106–2114. doi:10.1080/00958972.2019.1636975

Reddy, G. N., and Giri, S. (2016). Organic Heterocyclic Molecules Become Superalkalis. *Phys. Chem. Chem. Phys.* 18 (35), 24356–24360. doi:10.1039/C6CP04430A

Signorell, R., Palm, H., and Merkt, F. (1997). Structure of the Ammonium Radical from a Rotationally Resolved Photoelectron Spectrum. *J. Chem. Phys.* 106 (16), 6523–6533. doi:10.1063/1.473653

Silvi, B., and Savin, A. (1994). Classification of Chemical Bonds Based on Topological Analysis of Electron Localization Functions. *Nature* 371 (6499), 683–686. doi:10.1038/371683a0

Staroverov, V. N., Scuseria, G. E., Tao, J., and Perdew, J. P. (2003). Comparative Assessment of a New Nonempirical Density Functional: Molecules and Hydrogen-Bonded Complexes. *J. Chem. Phys.* 119 (23), 12129–12137. doi:10.1063/1.1626543

Sun, W.-M., Li, Y., Wu, D., and Li, Z.-R. (2013). Designing Aromatic Superatoms. *J. Phys. Chem. C* 117 (46), 24618–24624. doi:10.1021/JP408810E

Sun, W.-M., Wu, D., Kang, J., Li, C.-Y., Chen, J.-H., Li, Y., et al. (2018). Decorating Zintl Polyanions with Alkali Metal Cations: A Novel Strategy to Design Superatom Cations with Low Electron Affinity. *J. Alloys Compd.* 740, 400–405. doi:10.1016/J.JALLCOM.2017.12.075

Tkachenko, N. V., Sun, Z. M., and Boldyrev, A. I. (2019). Record Low Ionization Potentials of Alkali Metal Complexes with Crown Ethers and Cryptands. *ChemPhysChem* 20 (16), 2060–2062. doi:10.1002/CPHC.201900422

Tkachenko, N. V., Zhang, X. W., Qiao, L., Shu, C. C., Steglenko, D., Muñoz-Castro, A., et al. (2020). Spherical Aromaticity of All-Metal [$Bi@In_8Bi_{12}$]$^{3-/5-}$ Clusters. *Chem. Eur. J.* 26 (9), 2073–2079. doi:10.1002/CHEM.201905264

Tong, J., Li, Y., Wu, D., Li, Z.-R., and Huang, X.-R. (2011). Ab Initio Investigation on a New Class of Binuclear Superalkali Cations $M_2Li_{2k+1}{}^+$ ($F_2Li_3{}^+$, $O_2Li_5{}^+$, $N_2Li_7{}^+$, and $C_2Li_9{}^+$). *J. Phys. Chem. A.* 115 (10), 2041–2046. doi:10.1021/JP110417Z

Tong, J., Li, Y., Wu, D., Li, Z.-R., and Huang, X.-R. (2009). Low Ionization Potentials of Binuclear Superalkali B_2Li_{11}. *J. Chem. Phys.* 131 (16), 164307. doi:10.1063/1.3254835

Tong, J., Li, Y., Wu, D., and Wu, Z.-J. (2012). Theoretical Study on Polynuclear Superalkali Cations with Various Functional Groups as the Central Core. *Inorg. Chem.* 51 (11), 6081–6088. doi:10.1021/IC202675J

Tong, J., Wu, Z., Li, Y., and Wu, D. (2012). Prediction and Characterization of Novel Polynuclear Superalkali Cations. *Dalton Trans.* 42 (2), 577–584. doi:10.1039/C2DT31429K

Wang, Z.-C., Tkachenko, N. v., Qiao, L., Matito, E., Muñoz-Castro, A., Boldyrev, A. I., et al. (2020). All-metal σ-antiaromaticity in Dimeric Cluster Anion {[$CuGe_9Mes$]$_2$}$^{4-}$. *Chem. Commun.* 56 (48), 6583–6586. doi:10.1039/D0CC02525A

Weigend, F., and Ahlrichs, R. (2005). Balanced Basis Sets of Split Valence, Triple Zeta Valence and Quadruple Zeta Valence Quality for H to Rn: Design and Assessment of Accuracy. *Phys. Chem. Chem. Phys.* 7 (18), 3297–3305. doi:10.1039/B508541A

Conflict of Interest: The authors declare that the research was conducted in the absence of any commercial or financial relationships that could be construed as a potential conflict of interest.